New Chalcogenide-Based Hole Transport Materials for Colloidal Quantum Dot Photovoltaics

Eric Rong, Arlene Chiu, Christianna Bambini, Yida Lin, Chengchangfeng Lu, and Susanna M. Thon
The Johns Hopkins University, Baltimore, Maryland, 21218, United States

***Abstract*—Colloidal Quantum Dot (CQD) thin films are advantageous for solar energy generation because of their low-cost and size-tunable, solution-processable nature. However, their efficiency in solar cells is limited in part by the performance of the hole transport layer (HTL). Through Solar Cell Capacitance Simulations and Transfer Matrix Method calculations, we show that significant photogeneration occurs in the standard HTL of ethanedithiol-passivated lead sulfide CQDs which is a problem due to the sub-optimal carrier mobility in this material. We report new HTLs composed of chalcogenide-based materials to address these issues, and demonstrate an absolute power conversion efficiency improvement of 1.35% in the best device.**

A. Introduction

Lead Sulfide (PbS) colloidal quantum dots (CQDs) are advantageous for photovoltaic (PV) applications due to their size-tunable optical properties, their absorption in the infrared, and their inexpensive nature [1]. Their low-temperature material synthesis and solution-phase processability allow for facile thin-film fabrication techniques in scalable and flexible applications of solar energy technology, such as for building-integrated PV and wearable electronics, enabling new frontiers in the widespread adoption of renewable energy. Current state-of-the-art PbS CQD solar cell architectures, shown in Fig. 1a, are comprised of a fluorine-doped tin oxide (FTO) transparent conductive oxide contact, a zinc oxide (ZnO) nanoparticle-based electron transport layer (ETL), an absorbing layer of oleic acid-capped PbS CQDs that undergo a solution-phase ligand exchange with PbX_2 (X = Br, I) and ammonium acetate, a hole transport layer (HTL) of oleic acid-capped PbS CQDs that undergo a solid-phase ligand exchange with ethanedithiol (PbS-EDT), and a gold top contact [2].

However, PbS CQD-based solar cells exhibit limitations in efficiency, one source of which originates in the HTL [3]. The function of the HTL is to block electron transport, facilitate hole transport, prevent recombination, and to align the band structure of the absorbing layer with the deep work function metal top contact [3]. The highest efficiency PbS CQD solar cells utilize a thin (approximately 60 nm) PbS-EDT layer as the HTL [4], which exhibits low carrier mobility [5]. New methods of enhancing the transport characteristics of the HTL are thus desired to improve the performance of PbS CQD-based solar cells.

In this work, we use one-dimensional Solar Cell Capacitance Simulations (SCAPS-1D) [6] to determine the impact of the HTL electron mobility and hole mobility on device efficiency and Transfer Matrix Method (TMM) calculations to determine the absorption and generation profile of a solar cell. We then propose using chalcogenide-based materials to enhance the HTL carrier mobility and thus overall solar cell performance. In particular, we deposit a near-monolayer of tungsten diselenide (WSe_2), a 2D transition metal dichalcogenide (TMD), to act as the HTL. We characterized these solar devices with current density-voltage (JV) measurements to obtain solar cell performance metrics. The insights into the limitations of the PbS-EDT HTL and the improvements in the HTL that we demonstrate could be applied to developing new HTL materials or enhancing performance in CQD-based solar cells and other optoelectronic devices.

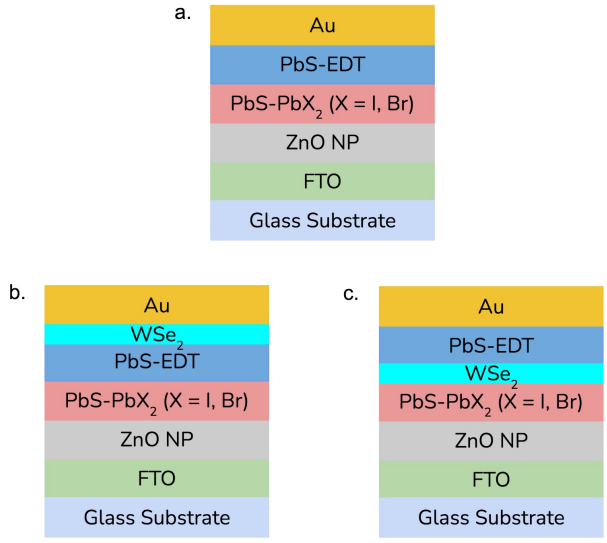

Fig. 1. (a) Structure of a state-of-the-art PbS CQD solar cell, with a PbS-EDT HTL. (b) Structure of a PbS CQD solar cell with an HTL that is augmented by a layer of WSe_2 between the PbS-EDT and the gold electrode. (c) Structure of a PbS CQD solar cell with an HTL that is augmented by a layer of WSe_2 between the absorbing layer and the PbS-EDT.

B. Experiments and Results

1) SCAPS Simulations: To better understand the factors inhibiting HTL performance and to determine the properties of a material that will improve it, we used SCAPS simulations to specifically look at the impact of electron mobility and hole mobility. For a structure with a 350 nm thick PbS-PbX_2 absorbing layer and a 60 nm thick PbS-EDT HTL, determined by empirical thickness optimization experiments, we used

National Science Foundation (DMR-1807342).

material parameters based on values from the literature [7]–[9]. We varied the electron mobility from 5 x 10^{-4} to 5 x 10^{-1} cm^2 V^{-1} s^{-1} and hole mobility from 5 x 10^{-5} to 5 x 10^{-2} cm^2 V^{-1} s^{-1}, which we determined based on values reported in the literature for PbS-EDT films [3].

Fig. 2 shows simulation results for the effect of HTL hole and electron mobility on power conversion efficiency (PCE) of the full solar cell. The electron mobility is kept constant at 5 x 10^{-3} cm^2 V^{-1} s^{-1} for the hole mobility calculations (blue asterisks), and the hole mobility is kept constant at 5 x 10^{-2} cm^2 V^{-1} s^{-1} for the electron mobility calculations (orange crosses). These constant values were chosen because they match the empirically measured hole and electron mobilities of our fabricated PbS-EDT HTL solar cells. From these results, we found that increasing both hole and electron mobility increased efficiency, so we were interested in developing a HTL material that exhibits both higher electron and hole mobility than PbS-EDT.

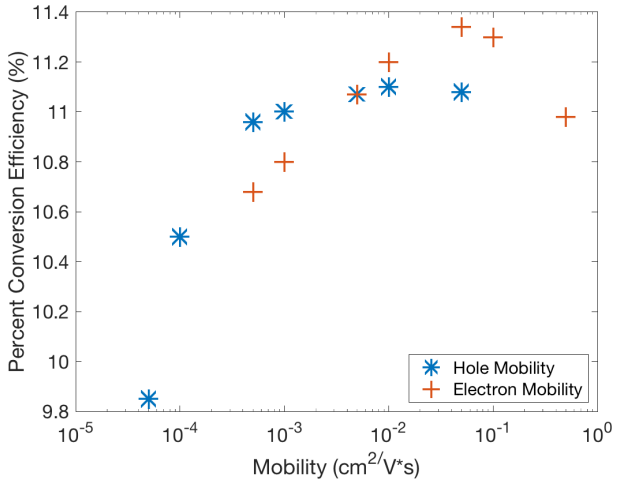

Fig. 2. SCAPS results for the effect of varying HTL mobility on solar cell efficiency. PCE when varying hole mobility (with constant electron mobility of 5 x 10^{-3} cm^2 V^{-1} s^{-1}) is given by the blue asterisks, and PCE when varying electron mobility (with constant hole mobility of 5 x 10^{-2} cm^2 V^{-1} s^{-1}) is given by the orange crosses.

The increased efficiency due to increased hole mobility was expected, as higher hole mobility should facilitate more effective hole transfer through the HTL. However, the existence of a region where increasing the electron mobility in the HTL resulted in increased PCE was less intuitive, since the HTL typically functions to block electron transfer. Past work has theorized that significant photogeneration can occur in the HTL [3]. This could explain the effect, since mobile carriers generated in the HTL would benefit from effective electron transfer through this layer to be collected as photocurrent [10]. We tested this theory by varying the thickness of the PbS-PbX_2 absorbing layer from $300 - 900$nm, as well as the HTL electron mobility from 5 x 10^{-4} to 5 x 10^{-2} cm^2 V^{-1} s^{-1} in simulations, and seeing if there was a point at which increased electron mobility ceased to improve the PCE. The results in Table I show that the device performance peaks at a PbS-PbX_2 thickness of around 500 nm, and that with absorbing layers thicker than 500 nm, increasing the HTL electron mobility ceased to impact overall device PCE. After that point, absorption in the HTL is negligible, and, therefore, high electron mobility does not significantly impact charge transfer. This explains why, for a sufficiently thick absorbing layer, electron mobility increases in the HTL do not impact PCE, which confirms our hypothesis.

TABLE I
SCAPS RESULTS FOR THE IMPACT OF ABSORBING LAYER THICKNESS AND HTL ELECTRON MOBILITY ON SOLAR CELL EFFICIENCY.

	Absorbing Layer Thickness (nm)							
HTL Electron Mobility (cm^2/Vs)	300	350	400	500	600	700	800	900
5e-4	10.3	11.1	11.6	11.9	11.9	11.7	11.6	11.4
5e-3	10.8	11.5	11.8	12.0	11.9	11.8	11.6	11.4
5e-2	11.1	11.6	11.9	12.0	11.9	11.7	11.6	11.4

2) Transfer Matrix Method Calculations: To further confirm that significant photogeneration occurs in the HTL, we performed TMM calculations to quantify the absorption and generation in the standard PbS-EDT HTL solar cell [11]. The results in Fig. 3 demonstrate that 10.2% of overall total optical absorption occurs in the HTL, with larger percentages at longer wavelengths. This shows that significant photogeneration happens in the HTL, further confirming the results of our SCAPS simulations.

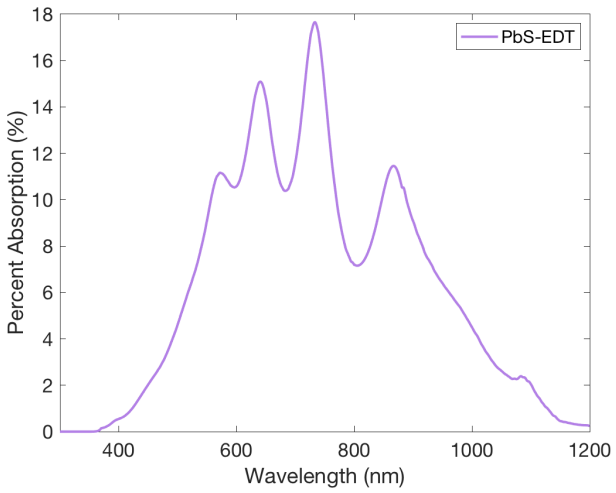

Fig. 3. Transfer Matrix Method calculations showing the wavelength-dependent absorption by the PbS-EDT HTL as a fraction of total device absorbance.

Because the fraction of light absorbed in the HTL contributes significantly to the overall power generation in the cell, we sought to enhance the performance of the PbS-EDT layer by increasing its hole and electron mobilities.

3) Energy Band Alignment: In addition to carrier mobility, the energy band structure of the HTL plays an important role in charge transfer and thus in device performance as well. We performed ultraviolet photoelectron spectroscopy (UPS)

measurements to determine the valence band edge locations of the absorbing layer and HTL, as well as ultraviolet-visible-near-infrared (UV-Vis-NIR) spectrophotometric measurements to determine the bandgap of each layer. We found that the valence band edge for the PbS-EDT HTL is approximately 0.07 eV shallower than that of the absorbing layer. Our SCAPS simulations indicated that the optimal valence band edge for the HTL should be 0.23 eV shallower than that of the absorbing layer [2]. Based on this, we sought a suitable material with higher hole mobility, electron mobility, p-type character and optimal band alignment.

Monolayer WSe_2 was identified as a promising candidate, with reported hole mobility of 250 cm^2 V^{-1} s^{-1}, electron mobility of 140 cm^2 V^{-1} s^{-1} [12], p-type doping [13], and similar band alignment to PbS-EDT, with valence band edges around -5.28 eV for PbS-EDT [3] and around -5.3 eV for WSe_2 [14].

4) Characterization: We fabricated solar cells with the structure described in the Introduction and shown in Fig. 1a. To introduce the WSe_2 into the structure, we used spin-casting to deposit a thin film of WSe_2 from the solution-phase. The solution consists of suspended nanoflakes ranging from approximately one to ten atomic layers in thickness with ethanol as the solvent, which were exfoliated using an ultra-sonicator, and then centrifuged for nanoflake size-selectivity [15]. We fabricated three solar cell structures; a standard structure with PbS-EDT as the HTL, a structure with a layer of WSe_2 between the absorbing layer and the PbS-EDT layer (Fig. 1c.), and a structure with a layer of WSe_2 between the PbS-EDT and Au layer (Fig. 1b.). Additionally, we fabricated structures using the same spin deposition process as devices made using WSe_2 solutions, replacing the WSe_2 solution with pure ethanol instead. This is meant to demonstrate if any impacts to performance result from the ethanol alone or from the WSe_2 solution in ethanol.

We then characterized these devices using JV measurements under simulated solar illumination to determine solar cell efficiency and related figures of merit. We obtained the results in Table II, with 16 and 47 devices tested per architecture. When comparing the WSe_2 devices to their pure ethanol counterparts, we notice an improvement in best device performance of the devices containing WSe_2, meaning that the presence of ethanol does not alone account for the performance increase. We also see that both structures containing WSe_2 perform better than the control in the best device, demonstrating that augmenting the PbS-EDT with a solution-processed WSe_2 layer improves solar cell performance, most noticeably through improvements in the fill factor. The slightly higher overall performance of the PbS-EDT/WSe_2 structure in comparison to the WSe_2/PbS-EDT structure may be explained by better band alignment with the absorbing layer.

TABLE II
SUMMARY OF EXPERIMENTAL CQD SOLAR CELL PERFORMANCE WITH AND WITHOUT WSe_2 IN THE HTL.

Structure	PCE [%] Best (Average)	Voc [V] Best (Average)	Jsc [mA/cm^2] Best (Average)	FF [%] Best (Average)
PbS-EDT	8.37 (7.3±0.56)	0.58 (0.58)	28.24 (24.97±1.61)	51.0 (50.0±1.6)
PbS-EDT/Ethanol	9.42 (8.08±1.31)	0.55 (0.53±0.05)	29.15 (26.53±1.91)	59.0 (57.0±3.73)
PbS-EDT/WSe_2	9.72 (7.95±1.37)	0.58 (0.56±0.06)	27.84 (25.76±2.03)	60.0 (54.0±5.3)
Ethanol/PbS-EDT	8.69 (7.69±0.72)	0.54 (0.53±0.03)	29.18 (26.32±1.80)	55.0 (55.0±0.53)
WSe_2/PbS-EDT	9.20 (7.92±0.98)	0.56 (0.55±0.02)	29.67 (26.31±1.81)	60.0 (54.3±4.4)

C. Conclusion

We performed SCAPS-1D simulations to identify the performance-limiting factors in CQD solar cell HTLs. We discovered that, paradoxically, increasing the electron mobility in the HTL correspondingly increased the efficiency of the overall solar cell, even though the HTL theoretically serves primarily to block electrons. We hypothesized that this could mean that significant photogeneration occurs in the HTL, so we investigated the influence of increasing the absorbing layer thickness to reduce the amount of HTL photogeneration. We found that increasing the HTL electron mobility ceases to improve the overall PCE when the absorbing layer thickness is greater than 500 nm, indicating that photogeneration does occur in the HTL. We confirmed these results with TMM calculations, which determined that approximately ten percent of the total device photogeneration occurs in the HTL, motivating the need for better hole and electron mobilities in the HTL. We hypothesized that augmenting the PbS-EDT HTL with a thin WSe_2 layer could improve hole and electron mobility while also having similarly compatible band alignment, thereby increasing overall solar efficiency. We found that our strategy increases the PCE of PbS CQD-based solar cells by 1.35% in the best device. Future work will involve developing HTLs consisting entirely of WSe_2 which should further improve PbS CQD solar cell PCEs.

ACKNOWLEDGMENT

The authors thank Hugo Celio for UPS measurements.

REFERENCES

[1] M. Hines and G. Scholes, "Colloidal PbS nanocrystals with size-tunable near-infrared emission: observation of post-synthesis self-narrowing of the particle size distribution," Adv. Mater., vol. 15, pp. 1844–1849, November 2003.

[2] M. Liu, O. Voznyy, R. Sabatini, F. P. García de Arquer, R. Munrir, A. H. Balawi et al., "Hybrid organic–inorganic inks flatten the energy landscape in colloidal quantum dot solids," Nat. Mater., vol. 16, pp. 258–263, February 2017.

[3] A. Chiu, E. Rong, C. Bambini, Y. Lin, C. Lu, and S. M. Thon, "Sulfur-infused hole transport materials to overcome performance-limiting transport in colloidal quantum dot solar cells," ACS Energy Lett., vol. 4, pp. 2897–2904, September 2020.

[4] M. J. Choi, F. P. García de Arquer, A. H. Proppe, A. Seifitokaldani, J. Choi, J. Kim et al., "Cascade surface modification of colloidal quantum dot inks enables efficient bulk homojunction photovoltaics," Nat. Commun., vol. 11, January 2020.

[5] Y. Lin, G. Ung, B. Qiu, G. Qian, S. M. Thon, "Integrated concentrators for scalable high-power generation from colloidal quantum dot solar cells," ACS Appl. Energy. Mater., vol. 1, pp. 2592–2599, June 2018.

[6] M. Burgelman, P. Nollet, and S. Degrave, "Modelling polycrystalline semiconductor solar cells," Thin Solid Films, vols. 361–362, pp. 527-532, February 2000.
[7] A. Sharma, R. S. Yadav, B. P. Pandey, "Performance analysis of PbS colloidal quantum dot solar cell at different absorption coefficient," J. Energy Environ. Sustain., vol. 7, pp. 32–35, January 2019.
[8] J. Ray, T. K. Chaudhuri, C. Panchal, K. Patel, K. Patel, G. Bhatt, P. Suryavanshi, "PbS-ZnO solar cell: a numerical simulation," J. Nano-Electron. Phys., vol. 9, pp. 03041-1–4, June 2017.
[9] X. Zhang, E. M. J. Johansson, "Reduction of. charge recombination in PbS colloidal quantum dot solar cells at the quantum dot/ZnO interface by inserting a MgZnO buffer layer," J. Mater. Chem. A, vol. 5, pp. 303–310, January 2017.
[10] A. Chiu, C. Bambini, E. Rong, Y. Lin, S. M. Thon, "New hole transport materials via stoichiometry-tuning for colloidal quantum dot photovoltaics," 2020 45th IEEE Phot. Spec. Conf. (PVSC), June 15th, 2020, pp. 1096–1097.
[11] G. F. Burkhard, E. T. Hoke, M. D. McGehee, "Accounting for interference, scattering, and electrode absorption to make accurate internal quantum efficiency measurements in organic and other thin solar cells," Adv. Mater., vol. 22, pp. 3293-3297, August 2010.
[12] W. Liu, W. Cao, J. Kang, K. Banerjee, "High-performance field-effect-transistors on monolayer WSe_2, ECS Trans., vol. 58, pp. 281-285, 2013.
[13] P. Zhao, D. Kiriya, A. Azcatl, C. Zhang, M. Tosun, Y. Liu et al., "Air stable p-doping of WSe_2 by covalent functionalization," ACS Nano, vol. 8, pp. 10808-10814, October 2014.
[14] Y. Liu, P. Stradins, S. Wei, "Van der Waals metal-semiconductor junction: weak Fermi level pinning enables effective tuning of Schottky barrier," Sci. Adv., vol. 2, April 2016.
[15] G. Kakavelakis, A.E.D.R. Castillo, V. Pellegrini, A. Ansaldo, P. Tzourmpakis, R. Brescia, M. Prato, E. Stratakis, E. Kymakis, and F. Bonaccorso, "Size-Tuning of WSe2 Flakes for High Efficiency Inverted Organic Solar Cells,", ACS Nano, vol. 11, pp. 3517-3531, February 2017.